

This is the accepted manuscript made available via CHORUS. The article has been published as:

## Floquet Spectrum and Transport through an Irradiated Graphene Ribbon

Zhengkao Gu, H. A. Fertig, Daniel P. Arovas, and Assa Auerbach

Phys. Rev. Lett. **107**, 216601 — Published 15 November 2011

DOI: [10.1103/PhysRevLett.107.216601](https://doi.org/10.1103/PhysRevLett.107.216601)

# Floquet Spectrum and Transport Through an Irradiated Graphene Ribbon

Zhenghao Gu<sup>1</sup>, H. A. Fertig<sup>1</sup>, Daniel P. Arovas<sup>2</sup>, and Assa Auerbach<sup>3</sup>

1. Department of Physics, Indiana University, Bloomington, IN 47405

2. Department of Physics, University of California at San Diego, La Jolla, CA 92093 and

3. Department of Physics, Technion, 32000 Haifa, Israel

Graphene subject to a spatially uniform, circularly-polarized electric field supports a Floquet spectrum with properties akin to those of a topological insulator, including non-vanishing Chern numbers associated with bulk bands and current-carrying edge states. Transport properties of this system however are complicated by the non-equilibrium occupations of the Floquet states. We address this by considering transport in a two-terminal ribbon geometry for which the leads have well-defined chemical potentials, with an irradiated central scattering region. We demonstrate the presence of edge states, which for infinite mass boundary conditions may be associated with only one of the two valleys. At low frequencies, the bulk DC conductivity near zero energy is shown to be dominated by a series of states with very narrow anticrossings, leading to super-diffusive behavior. For very long ribbons, a ballistic regime emerges in which edge state transport dominates.

PACS numbers: 72.80.Vp, 73.23.-b, 73.22.Pr

*Introduction and Key Results* – The electronic properties of graphene are very unusual among two-dimensional conducting systems, in large part because the low energy physics is controlled by two Dirac points, which form the Fermi surface of the system when undoped [1–3]. One of the very interesting possibilities for this system is that, with spin-orbit coupling, it may represent the simplest example of a topological insulator [4–6]. Topological insulators are systems for which the bulk spectrum is gapped, but which support robust, gapless edge states. Unfortunately, spin-orbit coupling in graphene appears to be too weak to allow observation of this behavior with currently available samples.

Very recently, theoretical studies have suggested that an analog of topological insulating behavior can be *induced* in graphene by a time-dependent electric potential [7–12]. The proposal entails exposing graphene to circularly-polarized electromagnetic radiation of wavelength much larger than the physical sample size, such that only the electric field has significant coupling to the electron degrees of freedom. The periodic nature of the field necessitates that the quantum states of the electrons are solutions of a Floquet problem, characterized by a “quasi-energy”  $\varepsilon_\alpha$  with allowed values in the interval  $[-\omega/2, \omega/2]$ , where  $\omega$  is the frequency of the radiation [13]. This same physics allows one to induce topological-insulating properties in a variety of systems that are otherwise only “almost” topological insulators [8]. Because time-reversal symmetry is explicitly broken in this system, it should support a Hall effect [7] which, when measured in an appropriate geometry, may be quantized [11].

A key challenge one faces in determining transport properties of this system is the assignment of electron occupations to the Floquet states. In general, the quasienergies  $\varepsilon_\alpha$  cannot be simply inserted as energies in a Fermi-Dirac distribution since they are limited to a finite interval of real values, determined by the frequency.

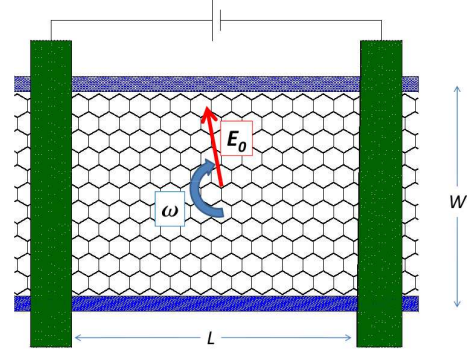


FIG. 1: (Color online) Schematic diagram of device geometry.

In this study, we assume Fermi-Dirac distributions only for the incoming waves far in the non-irradiated leads. Thus we assume that electrons are injected and removed from the system via highly doped, ideal leads in which any possible effects of an electric field have been screened out, and that the transport within the (finite) irradiated region is quantum coherent. Our geometry is a direct analog of one studied in Ref. 14 for the time-independent case, and is illustrated in Fig. 1. Identical leads are taken to be made of highly doped graphene. This leads to a vanishing time-averaged current in the absence of a DC bias, which avoids photovoltaic (charge pumping) effects.

For an infinite ribbon geometry, the momentum  $k_x$  along the ribbon axis is a good quantum number, and one may compute an effective band structure for the Floquet eigenvalue  $\varepsilon_\alpha$ . Fig. 2 illustrates this for several cases. Fig. 2(a) displays the bands closest to  $\varepsilon = 0$  for a relatively large frequency,  $\hbar\omega = 3t$  where  $t$  is the tight-binding hopping parameter. This result is illustrative for its relative simplicity, but is only relevant to very small system sizes for which the electric field may be approximated as uniform throughout the sample [11]. One

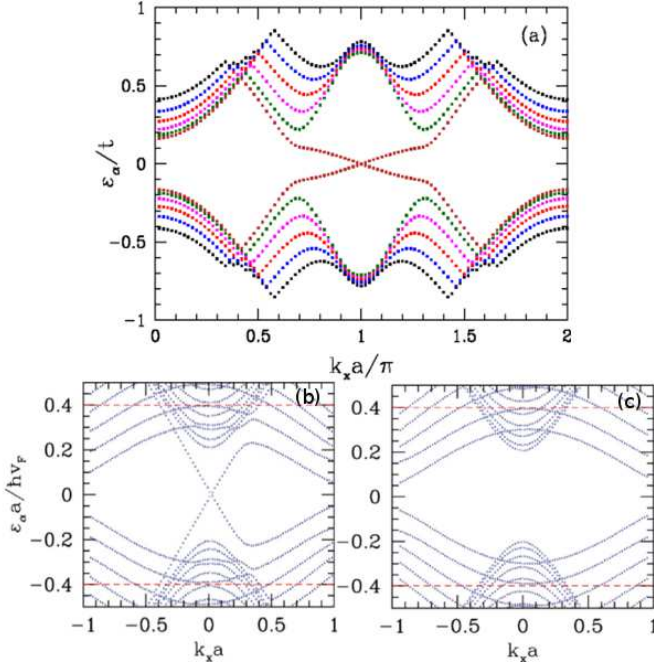


FIG. 2: (Color online) (a) Tight-binding Floquet spectrum as a function of  $k_x$  for a graphene ribbon oriented in the zigzag direction, subject to a circularly polarized electric field of magnitude  $E_0$  with  $eE_0a/\hbar\omega = 0.5$ ,  $\hbar\omega/t = 3.0$ , where  $a$  is the Bravais lattice constant and  $t$  the hopping parameter. (b,c) Spectra from Dirac equation with infinite mass boundary conditions, corresponding to two different valleys. Only one valley carries edge states. Frequency  $\omega a/v_F = 5$ , electric field amplitude  $E_0/\hbar\omega = 1$ , ribbon width  $W = 45a$ .

may see two sets of minima/maxima, corresponding to the two valleys, separated by a gap that does not vanish even as the system width  $W$  becomes very large. This intrinsic gap in the Floquet spectrum is an analog of that which opens in the presence of spin-orbit coupling for the static graphene system [4]. In further analogy to this, a pair of edge states traverses the gap and connects the two valleys, while (anti-)crossing around  $k_x = 0$ .

Figs. 2(b,c) illustrate corresponding results for Floquet spectra of two individual Dirac points subject to the circulating electric field, corresponding to the two different valleys, with infinite mass boundary conditions. In analogy with a topological insulator, one sees that both valleys develop gaps which do not go away as  $W$  becomes large, but only one supports edge states, so that the number of states at an edge is unaffected (modulo 2) by the change of boundary condition, while the details of how these states disperse are changed. Since the system with its edge state may be well-described qualitatively with just the single valley illustrated in Fig. 2(b), we focus our attention on this case for the transport calculations.

Fig. 3 illustrates typical results for the conductance of the system as a function of the scattering region length,  $L$ . At large  $L$  one can see the conductance level off to

a constant value, indicating the presence of edge states. For sufficiently wide samples this ballistic behavior will be robust against disorder, since states carrying current in opposite directions reside on opposite sides of the sample. The presence of a finite current for large  $L$  is in marked contrast to the behavior in the absence of the radiation, for which the conductance vanishes [14]. Surprisingly, the conductance exceeds the unirradiated conductance for all values of  $L$ , in spite of the fact that a gap has opened in the (Floquet) spectrum of the bulk system [7]. The explanation of this lies in the fact that Floquet eigenvalues are restricted to a finite interval, for example  $-\omega/2 < \varepsilon_\alpha < \omega/2$ , so that energy states outside this interval in the absence of the periodic potential are folded into it. For fixed  $k_y$ , this results in a series of repeated crossings at values of  $v_F k_x \approx m\omega$ , where  $m$  are non-zero integers. In a system without edges (i.e., if one considers periodic boundary conditions rather than a ribbon) these become avoided crossings with very small gaps, as we explain below, which transport current via evanescent states. Remarkably, transport through these states results in super-diffusive behavior,  $G \sim 1/L^b$ , with  $b < 1$ , as is apparent in Fig. 3. This non-analytic behavior reflects an explosive growth of the decay length of evanescent states with large  $|m|$ , which has the form

$$\xi_m \approx \left( \frac{|m|\omega}{A_0} \right)^{2|m|} \frac{e^{-\eta|m|}}{|m|\omega}, \quad (1)$$

where  $A_0 = E_0/\omega$  characterizes the electric field amplitude, assumed to be small, and  $\eta$  is a number of order unity. As we argue below, the rapid growth of  $\xi_m$  with  $m$  results in an anomalously large penetration of the electrons into the irradiated region.

*Transmission Through Irradiated Region* – The wavefunctions for Dirac electrons subject to circularly polarized radiation obey the time-dependent Schrödinger equation  $[-i\partial_t + \mathcal{H}] \Psi \equiv H_F \Psi = 0$ , where the Hamiltonian of the system has the form

$$\mathcal{H} = \begin{pmatrix} 0 & p_x - ip_y + A_x - iA_y \\ p_x + ip_y + A_x + iA_y & 0 \end{pmatrix} \quad (2)$$

where  $\mathbf{A} = A_0(\cos \omega t, \sin \omega t)$ , and  $p_{x,y} = -i\partial_{x,y}$ . (Note we have set the Fermi velocity  $v_F = 1$  in this expression.) Since  $\mathcal{H}$  is periodic in time, the solutions will be Floquet states, which have the form  $\Psi(\mathbf{r}, t) = e^{i\varepsilon_\alpha t} [\Phi_A(\mathbf{r}, t), \Phi_B(\mathbf{r}, t)]^T$ , with  $\Phi_\mu(\mathbf{r}, t+T) = \Phi_\mu(\mathbf{r}, t)$  and  $T = 2\pi/\omega$ . Adopting infinite mass boundary conditions leads to the conditions [14]  $\Phi_A(x, y=0, t) = \Phi_B(x, y=0, t)$  and  $\Phi_A(x, y=W, t) = -\Phi_B(x, y=W, t)$ . Eigenstates of  $\mathcal{H}$  which meet these boundary conditions are

$$\Phi^{(n,s)} = \frac{1}{\mathcal{N}_s} \left\{ \begin{pmatrix} sz^* - 1 \\ 1 - sz \end{pmatrix} e^{iq_n y} + \begin{pmatrix} 1 - sz \\ sz^* - 1 \end{pmatrix} e^{-iq_n y} \right\} \times e^{ik_x x - iA_y y}, \quad (3)$$

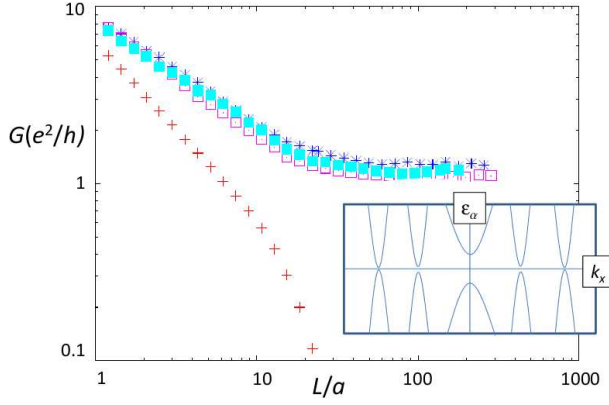


FIG. 3: (Color online) Conductance vs.  $L$  for several different bandwidths:  $q_{n_{\max}}W = \pi n_{\max}$ , with  $n_{\max} = 10$  (blue asterisks), 15 (lavender open squares), 25 (aqua closed squares). For these plots,  $W = 20a$ ,  $\omega a/v_F = 5$ , and number of time steps is 13. Note approximate power law behavior  $G \sim L^{-b}$  with  $b \approx 0.65$  for  $L < W$ . For comparison, results for  $E_0 = 0$  displayed as red crosses, displaying  $G \sim 1/L$  behavior for  $L < W$ . Inset: Illustration of  $\varepsilon_\alpha$  vs.  $k_x$  for infinite system with periodic boundary conditions, showing Floquet copies of spectrum and resulting avoided crossings for  $k_x \neq 0$ .

where  $z = (q_x + iq_n)/q$ ,  $q_x = k_x - A_x$ ,  $q_n = (n + \frac{1}{2})\pi/W$ ,  $s = \pm 1$ ,  $\mathcal{H}\Phi = sq\Phi$ , and  $\mathcal{N}_s$  is a normalization constant. States in the leads of the system are generated by setting  $\mathbf{A} = 0$  in Eq. 3.

Our strategy for finding the Floquet eigenvalues is to discretize time and expand the Floquet operator  $H_F$  in instantaneous eigenstates of the Hamiltonian  $\mathcal{H}$ . Writing  $\Phi^{(n,t_i,s)}(t) \equiv \Phi^{(n,s)}(t) \delta_{t_i,t}$ , we may then write  $\langle n_1, s_1, t_1 | \mathcal{H}(t) | n_2, s_2, t_2 \rangle = E_{(n_1,s_1)}(t_1) \delta_{n_1,n_2} \delta_{s_1,s_2} \delta_{t_1,t_2}$ . The Floquet operator can then be written as a matrix of the form

$$\begin{aligned} \langle n_1, s_1, t_1 | H_F | n_2, s_2, t_2 \rangle &= E_{(n_1,s_1)}(t_1) \delta_{t_1,t_2} \delta_{n_1,n_2} \delta_{s_1,s_2} \\ &- \frac{i}{2\Delta t} \left[ \langle n_1, s_1, t_1 | n_2, s_2, t_1 - \Delta t \rangle \delta_{t_2, t_1 - \Delta t} \right. \\ &\quad \left. - \langle n_1, s_1, t_1 | n_2, s_2, t_1 + \Delta t \rangle \delta_{t_2, t_1 + \Delta t} \right], \quad (4) \end{aligned}$$

whose eigenvalues are the allowed values of  $\varepsilon_\alpha$  for an infinite ribbon. Note that the states are implicitly functions of  $k_x$ . Diagonalization of Eq. 4 generates results such as those depicted in Fig. 2(b). These results were obtained for  $0 \leq n \leq 30$  and 19 time slices.

Turning to the conductance, in the leads there are no microwaves, so that eigenvalues of  $H_F$  with  $\mathbf{A} = 0$  have the form  $\varepsilon = \pm \sqrt{k_x^2 + q_n^2} + \sin(m\omega\Delta t)/\Delta t \equiv \pm E_n(k_x) + \varepsilon_m^t$ . This implicitly defines an equation for  $k_x$ , which depends on the integers  $n$  and  $m$ . In the scattering region as well, for a given subband of the Floquet spectrum, we need to know the values of  $k_x$  that will give some specified Floquet eigenvalue  $\varepsilon_\alpha$ . This is equivalent to finding the values of  $k_x$  where the bands illustrated in Fig. 2(b) cross some specified horizontal line. Note that if there is

no such crossing for a given band then the corresponding  $k_x$  is actually complex, indicating an evanescent state.

In order to match the wavefunctions in the leads to the scattering region we need to know these latter values of  $k_x$ , for a given Floquet eigenvalue  $\varepsilon_\alpha$ . To accomplish this we multiply the eigenvalue equation by  $\sigma_x$  to obtain

$$[(-i\partial_t - \varepsilon_\alpha)\sigma_x + i\sigma_z p_y] \vec{\psi} = k_x \vec{\psi}. \quad (5)$$

This is a non-Hermitian matrix equation which we approximately solve in a manner analogous to what we did for the original Floquet equation. Eigenvectors give us the wavefunctions in the scattering region, and the eigenvalues  $k_x$  that enter into the plane wave part of the wavefunction  $e^{ik_x x}$ . A comparison of these solutions to  $\varepsilon_\alpha(k_x)$  obtained by diagonalizing  $H_F$  reveals excellent agreement between the two calculations.

We now have analytic formulas for the wavefunctions in the leads, and approximate numerical solutions for them, represented in a finite basis of the states  $\Phi^{(n,s)}(y) e^{ik_x(n,m,s)x + imt}$ , in the scattering region. These need to be matched at two junctions. To accomplish this we match the wavefunctions on discrete points in  $y$ , taking  $y_j = (j + \frac{1}{2})W/(n_{\max} + 1)$ , where  $n_{\max} + 1$  is the number of transverse states retained, and  $j \in \{0, \dots, n_{\max}\}$ . This defines a set of linear equations which we solve numerically, and from which the matrix  $T_{qp}^{LR}(E, E + \varepsilon_n^t)$ , representing the time-averaged transmission across the structure, may be obtained. (Here  $q, p$  represent transverse channels in the left and right leads, respectively, and  $E$  is the energy of an impinging electron from the left.) One may show that by matching on these particular points one enforces current conservation in the solution; this is confirmed numerically to 1 part in  $10^3$ . The conductance is finally given by [15, 16]

$$G = \frac{e^2}{h} \sum_{p,q,n} T_{qp}^{LR}(E_F, E_F + \varepsilon_n^t) \quad (6)$$

where  $E_F$  is the Fermi energy in the leads.

*Evanescent Transmission in Irradiated System* – A prominent result from the calculations of the two-terminal conductance is an approximate power law behavior  $G \sim L^{-b}$  when  $L < W$ . As  $b$  is non-integral this represents non-analytic behavior, and the fact that it emerges well above the large  $L$  value of  $G$  suggests it is a result of evanescent state transport. This behavior turns out to be rather natural when one accounts for higher order crossings at non-zero  $k_x$  of the Floquet spectrum. In a realistic situation, for example if the impinging radiation is in the microwave regime,  $\hbar\omega \sim 10^{-3}$  eV, one will have many such crossings since the graphene bandwidth ( $\sim 10$  eV) is relatively large.

To demonstrate the behavior, we consider a simpler problem in which there is a half-space of irradiated graphene, and a half-space of highly-doped, unirradiated graphene, joined across  $x = 0$ , and we adopt periodic

boundary conditions in the transverse direction so that there are no edge states. For this situation  $k_y$  is a good quantum number. States with zero energy are perfectly backscattered in this case because there are no propagating states with zero Floquet eigenvalue. In the steady state situation there is a charge density tail penetrating the irradiated graphene, which has an approximate power law falloff with  $x$ .

To see this, we need to know how evanescent wavefunctions fall off with  $x$  inside the irradiated graphene. In the limit of vanishing microwave amplitude  $A_0$ , the Floquet spectrum will have pairs of states crossing  $\varepsilon_\alpha = 0$  at  $k_x = \pm k_m^0 = \pm \sqrt{(m\omega)^2 - k_y^2}$ . The degeneracy is lifted for non-vanishing  $A_0$ , which we take to be small compared to  $\omega$ . The resulting anti-crossing will occur at high order in perturbation theory, since the degeneracy occurs for states with time dependence  $\exp(\pm im\omega t)$ , whereas the perturbation  $V = A_0 (\sigma^x \cos \omega t + \sigma^y \sin \omega t)$  connects states whose frequencies differ by a single unit of  $\omega$ . Thus the gap that opens at the crossing will be proportional to  $(A_0/\omega)^{2m}$ . Since the inverse gap is essentially the localization length we wish to compute this. One approach is to use the resolvent operator  $\tilde{G}(z) = (z - \tilde{H}_F)^{-1}$  with  $\tilde{H}_F = \tilde{H}_0 + \tilde{V}$ . Poles of the  $2 \times 2$  matrix

$$\tilde{G} = \begin{pmatrix} \langle m, - | \hat{G} | m, - \rangle & \langle m, - | \hat{G} | -m, + \rangle \\ \langle -m, + | \hat{G} | m, - \rangle & \langle -m, + | \hat{G} | -m, + \rangle \end{pmatrix} \quad (7)$$

where  $s = \pm$  indicates a particle-like (+) or hole-like (-) state, are the eigenvalues of  $H_F$ . Expanding  $\tilde{G}$  in powers of  $\tilde{V}$  allows one to define a self-energy,  $\tilde{G}^{-1} = \tilde{G}_0^{-1} - \tilde{\Sigma} = z - \tilde{H}_0 - \tilde{\Sigma}$ , with  $\tilde{H}_0 = 0$  for the states of interest. The diagonal components of  $\Sigma$  simply shift the precise location of the anticrossing on the  $k_x$  axis and may be ignored. To lowest non-trivial order, the off-diagonal components are  $\Sigma_\pm = \langle m, - | \Sigma | -m, + \rangle = \langle -m, + | \Sigma | m, - \rangle^*$ , with

$$\Sigma_\pm = \left( \frac{(k_x + ik_y)A_0}{2k} \right)^{2m} \times \prod_{n=-m+1}^{m-1} \left[ \langle n, + | \hat{G}^{(0)} | n, + \rangle - \langle n, - | \hat{G}^{(0)} | n, - \rangle \right]. \quad (8)$$

Evaluating the matrix elements and setting  $z = 0$ , one finds  $|\Sigma_\pm| = A_0^{2m} (m\omega)^{1-2m} \prod_n \left[ \left( \frac{n}{m} \right)^2 - 1 \right]^{-1}$ . In the limit of large  $m$ , the product can be evaluated; noting that  $\xi_m^{-1} = 2|\Sigma_\pm|$ , one arrives at the estimate in Eq. 1 with  $\eta = 4(1 - \ln 2) \approx 1.227$ .

To see the connection with power law behavior, one needs to develop matching conditions at the  $x = 0$  interface with these wavefunctions. This is a tedious but in principle straightforward exercise [17], yielding the result that the contribution to the density from large  $n$  has the

time-averaged form

$$\rho(x) \sim \sum_n \left( \frac{A_0}{\omega\tau} \right)^{2n} e^{-x/\xi_n},$$

where  $\tau$  is of order unity, and depends on  $k_y$ . The sum may be estimated by assuming it is dominated by a single term at large  $n$  when  $x$  is large; maximization yields

$$n_{\max} = \frac{\ln(\omega x)}{y + 2\ell_n} + C$$

where  $C$  is independent of  $L$ ,  $\ell_n$  is a correction of order  $\ln[\ln(\omega x)]$ , and  $y = -2\ln(A_0/\omega) - \eta$ . Using this term to estimate the sum yields the result  $\rho(x) \sim (\omega x)^{2\ln(A_0/\omega\tau)/(y+2\ell_n)}$ . Since this is a weak function of  $k_y$  (through  $\tau$ ), we see that summing over the transverse modes should result in an approximate power law density tail. Such a fall-off is expected to lead to similar behavior in the transmission. It is interesting to note that the actual value of the exponent is relatively insensitive to  $\omega$  and  $A_0$ , since these enter only through logs; this is consistent with our results, for which the observed power tends to remain in the interval  $0.6 < b < 0.75$  over a variety of choices for  $\omega$  and  $A_0$ .

We conclude with some speculations about the effects of disorder. Because of the chiral nature of the edge states, it is clear that the saturation of conductance at large  $L$  should be present in the system unless the disorder is very strong, for which states associated with opposite edges may approach one another and allow backscattering. We also expect the high-order anticrossings to survive moderate disorder as an enhancement of the density of states near zero Floquet eigenvalue; this should lead to an increase in conductance due to the radiation as discussed above for the clean case. However the localization lengths of these states will presumably be shortened by disorder, which will likely modify the precise form of the conductance as a function of  $L$ . We leave a detailed study of these effects to future research.

In summary, two-terminal transport through an undoped graphene ribbon subject to a circularly rotating electric field has a conductance that reveals the unusual nature of the Floquet spectrum of this system. Evanescent transport through relatively short ribbons is superdiffusive due to a series of near crossings with very small gaps. At larger ribbon lengths, transport becomes ballistic, revealing the presence of edge states which are a hallmark of the topological nature of the spectrum.

*Acknowledgements* – This work was supported by the NSF through Grant Nos. DMR-1005035 (HAF) and DMR-1007028 (DPA), and the US-Israel Binational Science Foundation (AA and DPA). We acknowledge the hospitality of the Aspen Center for Physics where this work was initiated. The authors thank Erez Berg, Luis Brey, Fernando de Juan, Netanel Lindner and Gil Refael for helpful discussions.

- 
- [1] A. H. Castro Neto, F. Guinea, N. M. R. Peres, K. S. Novoselov, and A. K. Geim, *Rev. Mod. Phys.* **81**, 109 (2009).
  - [2] N. Peres, *Rev. Mod. Phys.* **82**, 2673 (2010).
  - [3] S. Das Sarma, S. Adam, E. H. Hwang, and E. Rossi, *Rev. Mod. Phys.* **83**, 407 (2011).
  - [4] C. L. Kane and E. Mele, *Phys. Rev. Lett.* **95**, 146802 (2005).
  - [5] M. Z. Hasan and C. L. Kane, *Rev. Mod. Phys.* **82**, 3045 (2010).
  - [6] X. L. Qi and S. C. Zhang, arXiv:1008.2026.
  - [7] T. Oka and H. Aoki, *Phys. Rev. B* **79**, 081406(R) (2009).
  - [8] N. H. Lindner, G. Refael, and V. Galitski, arXiv:1008.1792.
  - [9] O. Roslyak, G. Gumbs, and D. Huang, arXiv:1101.5466.
  - [10] T. Kitagawa, E. Berg, M. Rudner, and E. Demler, *Phys. Rev. B* **82**, 235114 (2010).
  - [11] T. Kitagawa, T. Oka, A. Brataas, L. Fu, and E. Demler, arXiv:1104.4636.
  - [12] H. L. Calvo, H. M. Pastawski, S. Roche, and L. E. F. Foa Torres, arXiv:1105.2327.
  - [13] M. Razavy, *Quantum Theory of Tunneling* (World Scientific, New Jersey, 2003).
  - [14] J. Tworzydło, B. Trauzettel, M. Titov, A. Rycerz, and C. W. Beenakker, *Phys. Rev. Lett.* **96**, 246802 (2006).
  - [15] S. Datta, *Electronic Transport in Mesoscopic Systems* (Cambridge University Press, New York, 1997).
  - [16] In a general structure subject to a time-dependent potential there may be current even in the absence of DC bias across the system. One may show for that this is not the case the case for this structure, so that for small biases  $V$  the time-averaged current is  $GV$ .
  - [17] H. A. Fertig, unpublished.